Journal of the Geological Society, London, Vol. **162**, 2005, pp. 299–314. Printed in Great Britain.

Separation of Palaeogene and Neogene uplift on Nuussuaq, West Greenland

PETER JAPSEN[1], PAUL F. GREEN[2] & JAMES A. CHALMERS[1]

[1]*Geological Survey of Denmark and Greenland (GEUS), Øster Voldgade 10, DK-1350 Copenhagen K, Denmark (e-mail: pj@geus.dk)*

[2]*Geotrack International, 37 Melville Road, West Brunswick, Vic. 3055, Australia*

Abstract: The geological record exposed on Nuussuaq, central West Greenland, shows that uplift in the Palaeocene, probably caused by impact of the Iceland plume head, was followed by kilometre-scale subsidence. Analysis of apatite fission-track and vitrinite-reflectance data from borehole samples down to 3 km depth reveals that the samples cooled from maximum palaeotemperatures between 40 and 30 Ma followed by two further cooling episodes beginning in the intervals 11–10 and 7–2 Ma. When the first cooling episode began, the samples from the neighbouring Gro-3 and Gane-1 boreholes were buried 1500–2000 m deeper than at the present day, and the palaeogeothermal gradient was 40–48 °C km^{-1}. It is not clear whether this cooling involved exhumation or if it was due solely to reduction in heat flow and a drop in surface temperature. The two later episodes definitely involved exhumation because by then the palaeogeothermal gradient had declined to a value close to the assumed present value of 30 °C km^{-1}, which agrees with estimates from offshore wells. The most recent cooling episode corresponds to the incision of the present-day relief (*c*. 1100 m) below the summits around the two boreholes. We conclude that the present-day high mountains of West Greenland were not uplifted during the Palaeogene, but are erosional remnants of a landmass uplifted during the Neogene.

Keywords: West Greenland, Cenozoic, uplift, exhumation, fission-track dating.

Studies of the Cenozoic uplift and erosion of the passive continental margins around the North Atlantic commonly show evidence for multiple episodes of uplift (see Japsen & Chalmers 2000; Doré *et al*. 2002). Scandinavia appears to have been uplifted at least twice, in the Palaeogene (e.g. Faleide *et al*. 2002; Lidmar-Bergström & Näslund 2002; Nielsen *et al*. 2002) and again in the late Neogene (Riis & Fjeldskaar 1992; Rohrman *et al*. 1995; Faleide *et al*. 2002; Japsen *et al*. 2002; Lidmar-Bergström & Näslund 2002). Many studies of the British Isles have focused on Palaeogene uplift (e.g. Green 1986; White & Lovell 1997; Jones *et al*. 2002) but there is ample evidence that uplift and erosion also affected the British Isles during the late Cenozoic (e.g. George 1966; Green 1989, 2004; Japsen 1997; Green *et al*. 2001*b*; Stoker 2002). Whereas Palaeogene uplift has been related to the impact of the Iceland plume during the Palaeocene and the opening of the North Atlantic during the Eocene, the causes of late Cenozoic vertical movements in the region remain obscure.

The difficulty in resolving both the timing and magnitude of the Cenozoic phases of vertical movements is probably the most critical obstacle in recognizing their nature and hence in understanding their causes. Such movements are frequently ignored because they are manifested by removal of sedimentary cover and have led to exhumation of rocks that were formed long before the onset of erosion, giving the impression that no cover was ever deposited. For example, for many years the present-day mountains in both Scotland and Scandinavia were thought of as being the worn stumps of the much higher mountain range formed during the Caledonian orogeny *c*. 400 Ma ago instead of being recognized as blocks of crust uplifted to their present elevations during the Cenozoic (e.g. Rohrman *et al*. 1995; Thomson *et al*. 1999*b*). Indeed, the lack of a generally accepted hypothesis to explain the presence of mountains in Norway has been termed 'the Scandinavian enigma'.

West Greenland has also been subjected to uplift during the Cenozoic, in a similar way to NW Europe (Mathiesen 1998; Chalmers 2000). One difference is that the exposed Nuussuaq Basin in central West Greenland contains a detailed record of early Palaeogene uplift and erosion followed by rapid subsidence and infilling by volcanic rocks and sediments (Figs. 1 and 2) (e.g. Pedersen *et al*. 1993, 2002*b*; Dam *et al*. 1998; Chalmers *et al*. 1999). This record allows separation of the effects of Palaeocene–Eocene uplift or subsidence, evident in the sedimentary and volcanic succession, from later events that lifted Palaeocene marine sediments to their present heights of over a kilometre above sea level (Fig. 3) (Piasecki *et al*. 1992). However, the precise timing of uplift remains uncertain.

In this study, we have used new apatite fission-track analyses (AFTA®; see Green *et al*. 2002) and vitrinite-reflectance (VR) data from two boreholes through lower Palaeocene and Mesozoic sediments on Nuussuaq, combined with geological and topographical constraints, to show that kilometre-scale uplift and erosion occurred during the late Neogene, probably in two discrete phases. We think this may be the first time that it has been possible to separate the effects of Palaeogene and Neogene uplift so clearly because the effects of the Palaeogene phase can be studied in the preserved succession that is now exposed as a result of the Neogene uplift.

Palaeogene uplift and subsidence in central West Greenland

Nuussuaq Basin onshore

Cretaceous and lower Palaeocene sediments partly covered by Palaeocene–Eocene picritic and basaltic lavas are exposed in the Nuussuaq Basin on the island of Disko and the peninsulas of

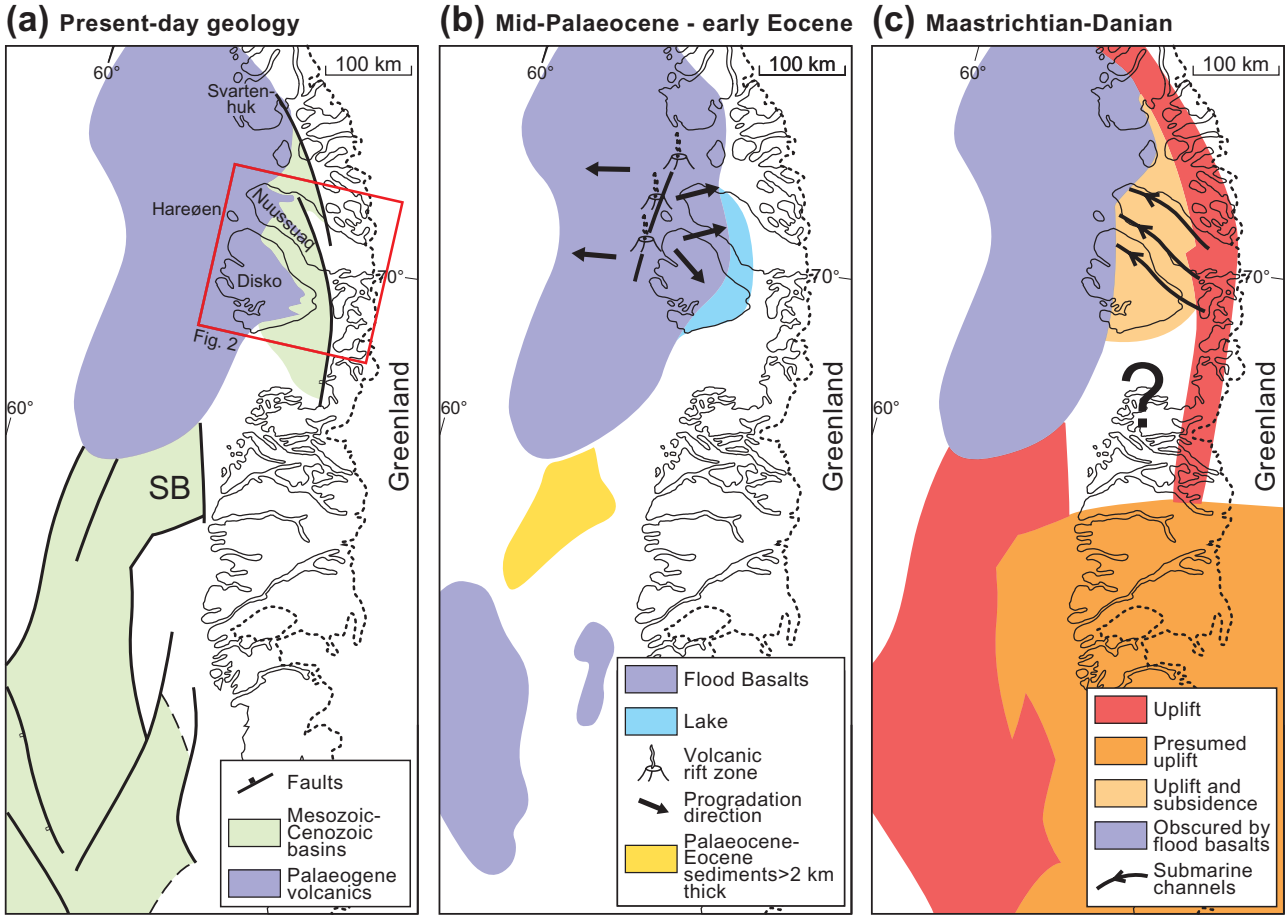

Fig. 1. (**a**) Place names and sedimentary basins in central West Greenland. SB, Sisimiut Basin (offshore). Rectangle indicates main part of the Nuussuaq Basin and location of map in Figure 2. (**b**) Palaeogeography during mid-Palaeocene to early Eocene times. Three areas of volcanism are known, the northernmost of which extends offshore from the well-known exposures onshore. Basalts and picrites flowed both east and west from a rift zone just west of Disko and Nuussuaq (Skaarup 2002). The Nuussuaq Basin was undergoing rapid subsidence and the accommodation space was being filled by sediments and a hyaloclastite delta that prograded eastwards. Rapid subsidence in the Sisimiut Basin created accommodation space that was filled by over 2 km of deltaic sediments that prograded southwards (Dalhoff *et al*. 2003). (**c**) Palaeogeography during late Maastrichtian to Danian time. The Nuussuaq Basin on Disko and Nuussuaq was subject to two phases of uplift with an intervening period of subsidence and sedimentation (Dam *et al*. 1998). No evidence of the period of subsidence has been preserved in the sedimentary basins offshore south of the basalts (Dalhoff *et al*. 2003).

Nuussuaq and Svartenhuk (Fig. 1) (Clarke & Pedersen 1976; Chalmers *et al*. 1999; Henriksen *et al*. 2000).

Two phases of valley incision have been observed beneath the flood basalts in the Nuussuaq Basin (Dam & Sønderholm 1998; Dam *et al*. 1998; Dam & Nøhr-Hansen 2001; Dam 2002). The earliest channels were formed during the latest Maastrichtian, and Dam *et al*. (1998) suggested that they were eroded as submarine canyons on the footwalls of fault blocks formed during an episode of extensional tectonism (Chalmers *et al*. 1999). The later channels were eroded subaerially during the mid-Palaeocene in an area undergoing uplift probably in response to the impact of the head of the Iceland plume (Dam *et al*. 1998). Volcanism commenced shortly after infilling of the later channels, during magnetochron 27n (Riisager & Abrahamsen 1999), corresponding to 61.3–60.9 Ma (Berggren *et al*. 1995).

Volcanism started on a submarine slope to the west of the area where the major channels were eroded. The volcanic pile built up above sea level so that lavas began to be erupted subaerially. However, at the shoreline the lavas entered the sea and formed eastward-prograding Gilbert-type delta structures with cross-bedded hyaloclastite sets up to 700 m thick (Pedersen *et al*. 1993), indicating that the basin had already subsided at least that much below contemporary sea level. The basin continued to subside during subsequent deposition of a 200 m thick succession of subaerial lavas alternating with five horizons of foreset-bedded hyaloclastites on Nuussuaq (Pedersen *et al*. 2002*b*), a succession recording an almost perfect balance between aggradation of the lava plateau and subsidence of the basin. This succession is overlain by a 160–180 m thick zone of subaerial lavas across which the transition from magnetochron 27n to 26r is recorded (Riisager & Abrahamsen 1999; Pedersen *et al*. 2002*b*), and above which Piasecki *et al*. (1992) found marine dinoflagellates at a present-day height of 1176 m above sea level.

Thus the latest Maastrichtian and Palaeocene sedimentary and volcanic rocks in the Nuussuaq Basin record an uplift event that Dam *et al*. (1998) estimated to be up to 1.3 km, followed by subsidence of at least 1000 m and probably considerably more than that. At least 900 m of this subsidence took place during magnetochron 27n (Pedersen *et al*. 2002*b*), which lasted 300 ka

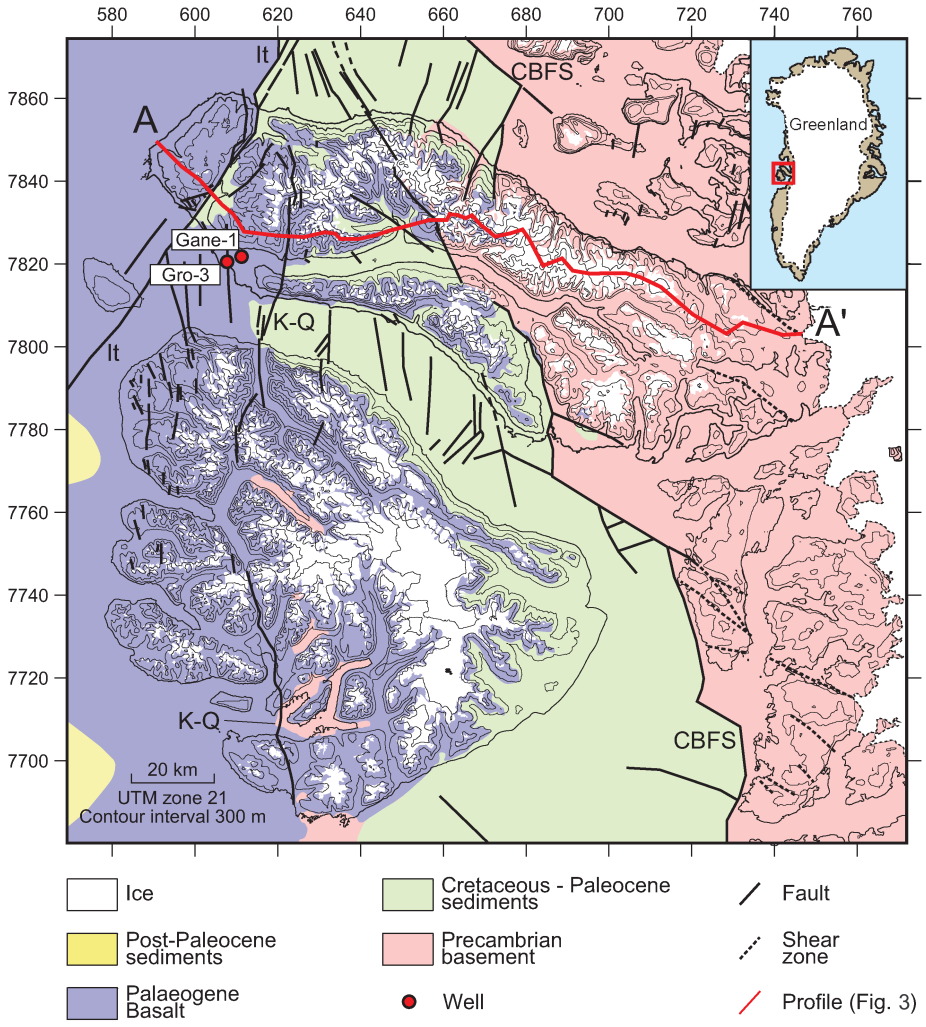

Fig. 2. Geology and onshore topography of the study area, and location of profile AA' (Fig. 3). The Gane-1 and Gro-3 wells are located at the mouth of a steep-sided valley with adjacent summits reaching elevations of *c*. 1100 m in Palaeocene volcanic rocks. Thus a succession of volcanic rocks of at least this thickness must once have covered the present-day ground surface. CBFS, Cretaceous Boundary Fault System; It, Itilli fault; K-Q, Kuugannguaq–Qunnilik fault. Topographical data from a digital terrain model, 250 m grid. Geology after Chalmers *et al*. (1999). Modified after Bonow 2004.

(Berggren *et al*. 1995), so the minimum subsidence rate was 0.3 cm a^{-1}.

Sisimiut Basin offshore

Dalhoff *et al*. (2003) have shown the presence of a major unconformity that separates mid-Palaeocene and younger sediments from Campanian and older sediments over the whole of the sedimentary basins offshore southern West Greenland (Fig. 1). They attributed this unconformity to uplift and erosion caused by impact of the head of the Iceland plume, because renewed sedimentation onto the unconformity (and presumably therefore

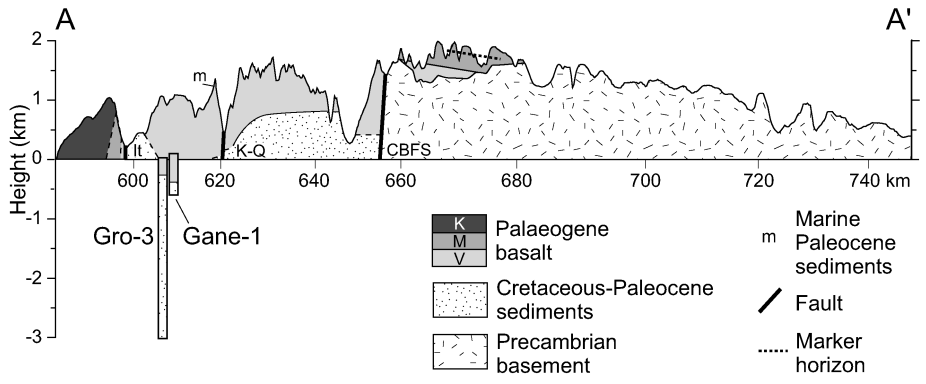

Fig. 3. Profile along Nuussuaq with projections of the stratigraphy in the Gane-1 and Gro-3 wells, SW of the profile and offset by 5–10 km (location in Fig. 2). Post-Palaeocene uplift of at least 1200 m is evident from the occurrence of marine Palaeocene sediments at that height (Piasecki *et al*. 1992). UTM zone 21 easting along horizontal axis. Basalt: K, Kanisut Mb, *c*. 53 Ma; M, Maligât Fm, *c*. 60 Ma; V, Vaigat Fm, *c*. 61 Ma (Storey *et al*., 1998). Marker horizon: Niaqussat and Nordfjord members (Maligât Fm). CBFS, Cretaceous Boundary Fault System; It, Itilli fault; K-Q, Kuugannguaq–Qunnilik fault. Geology after Rosenkrantz *et al*. (1974), Hald (1976), Piasecki *et al*. (1992), Garde (1994) and Pedersen *et al*. (2002*a*).

renewed subsidence) started contemporaneously with the onset of volcanism in the Nuussuaq Basin.

There was an episode of block faulting offshore that has been dated by drilling as having taken place between the Late Campanian and late Palaeocene (Aram 1999; Christiansen *et al*. 2001; Dalhoff *et al*. 2003), similar to the onshore episode suggested by Dam *et al*. (1998) and Chalmers *et al*. (1999). On the other hand, there appears to be no record preserved offshore (Dalhoff *et al*. 2003) of any equivalent of the Maastrichtian and Danian sediments onshore that record the details of the mid-Palaeocene uplift and subsidence. This can be most easily explained if erosion in the present offshore region during the Palaeocene episode of uplift (impact of the Iceland plume) was so extensive that it removed all traces of any Maastrichtian and early Palaeocene sedimentation, in contrast to what happened in the present-day onshore area.

The formation of the base Cenozoic unconformity offshore was followed by subsidence that created sufficient accommodation space in the Sisimiut Basin to contain a 2.5 km thickness of sediment deposited during 21 Ma of late Palaeocene to mid-Eocene time (Fig. 1) (Dalhoff *et al*. 2003). Seismic sequence analysis calibrated by borehole control shows that sedimentation in the northern part of the basin was constantly sufficient to fill the available accommodation space, indicated by the continuous deposition of delta-top facies. This indicates a subsidence rate of 0.1 cm a^{-1}.

These sediments were subsequently tilted and their landward margin was eroded by an unconformity that Chalmers (2000) called the 'base Quaternary' unconformity, the age of which is not well constrained. The late tilting of the Sisimiut Basin resembles the tilting and uplift that exposed the Nuussuaq Basin (compare Chalmers 2000, figs 3 and 4).

Thus the sedimentary and volcanic record preserved both onshore and offshore West Greenland shows evidence for substantial uplift associated with the impact of the Icelandic plume in the mid-Palaeocene, but indicates that this uplift was short lived and was followed by rapid and substantial subsidence. This uplift event could not therefore have been what formed today's West Greenland mountains. That event must have taken place later than the mid-Eocene, and probably took place much later. To investigate this we have modelled the thermal and exhumation history of the Nuussuaq Basin.

Principles of thermal history reconstruction

To assess the burial and denudation history of the area, we have used thermal history reconstruction, based on application of AFTA and VR data (e.g. Green *et al*. 2001*a*, *b*, 2002; Crowhurst *et al*. 2002). This approach makes it possible to identify the timing and magnitude of the main episodes of heating and cooling that have affected a sedimentary section. The variation of palaeotemperature through the section in each episode then allows key parameters such as palaeogeothermal gradients and amounts of missing section to be determined and the causes of heating and cooling to be evaluated (e.g. Bray *et al*. 1992; Duddy *et al*. 1994; Green *et al*. 1995).

Both AFTA and VR data are largely determined by maximum temperature. For this reason, extraction of thermal history information from AFTA and VR data begins by constructing a 'default thermal history', by combining the burial history derived from the preserved sedimentary section with the present-day geothermal gradient. If the observed data are consistent with the values predicted from this history, then the sample is at present at or close to its maximum post-depositional temperature, and the data retain little or no information on any palaeothermal effects. If, however, the data show a greater degree of fission-track annealing or VR maturity than expected on the basis of the default history, the sample must have been hotter in the past. In this case, AFTA provides an estimate of the time at which cooling began, and both AFTA and VR constrain the magnitude of the maximum palaeotemperature reached by individual samples. AFTA can also provide constraints on subsequent episodes of cooling from a lower palaeotemperature peak, through shortening of tracks formed after the earlier, maximum palaeotemperature episode. Data from a single sample can provide constraints on up to three discrete cooling episodes, if they are sufficiently separated in time and temperature (Green *et al*. 2001*a*). The annealing kinetics of fission tracks in apatite depends on the chlorine content of the apatite grains (Green *et al*. 1986). Incorporation of this variation in Cl content within each sample is essential in extracting correct thermal history information from AFTA data (e.g. Argent *et al*. 2002; Crowhurst *et al*. 2002). We do not attempt to constrain the whole thermal history of each sample. Instead, we focus on those key aspects of the thermal history that control the development of the AFTA parameters and VR values, specifically the maximum palaeotemperature of each sample and the time at which cooling from that palaeotemperature began.

Determination of maximum palaeotemperatures over a range of depths allows the palaeogeothermal gradient at the onset of cooling to be determined. Extrapolation of this palaeogeothermal gradient to an assumed palaeosurface temperature allows the amount of missing section to be estimated (see Bray *et al*. 1992; Green *et al*. 2002). 'Missing section' is the amount of section that has been removed from above a particular sample horizon after the time at which cooling commenced. A useful alternative approach is to regard such estimates as 'additional palaeoburial'.

Well data

The Gane-1 well (ground level 114 m above sea level (a.s.l.); see Fig. 2) was drilled as a slim-core borehole to 707 m in 1995 and encountered 500 m of Palaeocene volcanic rocks underlain by a sedimentary succession of Palaeocene age (Christiansen *et al*. 1996*a*; Nøhr-Hansen *et al*. 2002). VR data are available over a limited depth interval (Table 1) (Christiansen *et al*. 1996*b*). The Gro-3 hydrocarbon exploration well (ground level 22 m a.s.l.) was drilled to 2996 m in 1996, 4 km from the site of Gane-1, and encountered 303 m of Palaeocene volcanic rocks underlain by a sedimentary succession intersected by igneous intrusions whose cumulative thickness was 145 m (Christiansen *et al*. 1999). The sediments down to *c*. 1500 m depth have been dated as Coniacian–Danian, but it was not possible to date the deeper, *c*. 1500 m thick sedimentary succession because of thermal alteration (Nøhr-Hansen 1997). A well-developed, depth-dependent VR maturity trend (see note added in proof) is observed throughout the succession penetrated; the VR trend is remarkably regular and shows no sign of anomalies caused by intrusions or changes in gradient across possible unconformities (Table 1) (Bojesen-Koefoed *et al*. 1997).

Eight samples of sandstone for AFTA were taken from cores and cuttings in the depth range from 0.4 to 2.9 km below sea level in the Gane-1 and Gro-3 wells (Table 2; Fig. 4). The apatite yield was excellent in seven samples and good in one, but we have filtered the data from the Gro-3 borehole to eliminate the effects of spurious apatite grains that appear to represent contamination of the cuttings material. Some samples

Table 1. *Maximum palaeotemperatures from VR data*

Well name	Average depth (m)	Present temperature (°C)	Measured VR* (%)	Maximum palaeotemperature†‡ (°C)
Gane-1	503	15	0.70	116
Gane-1	510	15	0.66	109
Gane-1	526	16	0.69	115
Gane-1	535	16	0.70	116
Gane-1	547	16	0.67	111
Gane-1	591	18	0.75	122
Gane-1	615	18	0.68	113
Gane-1	635	19	0.58	96
Gane-1	641	19	0.60	99
Gane-1	649	19	0.72	118
Gro-3	370	11	0.77	124
Gro-3	510	15	0.74	121
Gro-3	1110	33	0.98	141
Gro-3	1150	35	1.01	143
Gro-3	1250	38	1.32	161
Gro-3	1300	39	1.23	156
Gro-3	1390	42	1.23	156
Gro-3	1545	46	1.42	166
Gro-3	1725	52	1.61	175
Gro-3	2365	71	2.24	198
Gro-3	2435	73	2.29	200

*Measured VR values from Christiansen *et al*. (1996*b*) and Bojesen-Koefoed *et al*. (1997).
†All estimates of maximum palaeotemperature were determined using assumed heating rates of 1 °C Ma^{-1} and cooling rates of 10 °C Ma^{-1}.
‡Maximum palaeotemperatures derived from VR data using the algorithm of Burnham & Sweeney (1989).

contained only small numbers of confined track lengths because of the low spontaneous track densities resulting from the recent cooling from >110 °C, and sample GC883-13 contained none. Apatites separated from samples for this study show distributions of Cl contents similar to those found in detrital apatites from common sandstone samples around the world, with the majority of grains having Cl contents between 0 and 0.1 wt% and a smaller number of grains containing up to 0.5 wt%, although a minor component of grains with Cl content up to 1 wt% is present in some samples. Full details of the AFTA data in these samples and in a larger dataset from the Nuussuaq Basin, and the associated thermal history interpretations, have been described by Green (2003) and this report is available from the Society Library or the British Library Document Supply Centre, Boston Spa, Wetherby, West Yorkshire LS23 7BQ, UK as Supplementary Publication No. SUP 18212 (250 pages). It is also available online at http://www.geolsoc.org.uk/SUP18212.

No present-day temperature information is available from these boreholes, so a present-day thermal gradient of 30 °C km^{-1} has been assumed. This value is in agreement with values in the range from 24 to 34 °C km^{-1} found for five wells offshore West Greenland based on borehole temperature data (Rolle 1985) tied to a sea-bed temperature of 2 °C and constrained on the basis of AFTA and VR results (Gibson 1999). The trend of the age data in Figure 4 towards zero at depths >3 km and the consistency between this and the predicted age–depth trends for the most sensitive (i.e. low-Cl) apatites suggests that this value is approximately correct.

Thermal history reconstruction for Gro-3 and Gane-1 boreholes

Thermal history interpretation of AFTA and VR data

We have analysed the Gro-3 and Gane-1 results together, assuming that the two well sites, only 4 km apart, were subjected to the same thermal history. The consistency of the results between the two boreholes suggests that this assumption is justified (Tables 1 and 2). The AFTA results from the boreholes define a highly consistent trend in which fission-track ages decrease with depth and are much less than the values predicted from the 'default thermal history' (Fig. 4). This shows that the sampled sedimentary units have been much hotter in the past.

Estimates of the peak palaeotemperatures attained by each sample in one or two palaeoheating episodes, together with the timing at which cooling from that peak began, are listed in Table 2. These estimates have been obtained by comparing measured AFTA parameters (fission-track age and track length distribution and their variation with Cl content) with the values predicted from a range of thermal histories. Using software that examines the degree of agreement between predicted and measured fission-track age and the track length distribution as a function of chlorine content, for an input thermal history, a best-fit solution is defined on the basis of maximum likelihood theory (similar to that described by Gallagher 1995). By systematically varying the timing of the onset of cooling and the peak palaeotemperature about the best-fit values, the range of conditions can then be defined for which the modelled parameters are consistent with the measured data within 95% confidence limits.

Identification of palaeothermal episodes

Synthesis of the timing constraints for individual cooling episodes identified from AFTA in each sample (Table 2), based on comparing the overlap of timing constraints from individual samples, suggests that three discrete palaeothermal episodes of cooling are required to explain the AFTA data in all samples, with cooling beginning in the following intervals (Fig. 5): 44–25 Ma (Eocene–Oligocene, henceforth referred to as 'Eocene–Oligocene'); 13–10 Ma (Late Miocene, or 'Miocene'); 7–2 Ma (latest Miocene to Pliocene, or 'Pliocene'). It should be noted that these intervals represent the range of uncertainty of times at which cooling began, and we do not suggest that cooling was

Table 2. *AFTA data and palaeotemperature analysis summary*

Sample no.	Depth (m)	Stratigraphic age (Ma)	Present temperature* (°C)	Fission track age† (Ma)	$P(\chi^2)$, no. of grains	Mean track length (μm)	S.D. (μm), number of track lengths	'Eocene–Oligocene'		'Miocene'		'Pliocene'	
								Maximum palaeotemperature‡ (°C)	Onset of cooling‡ (Ma)	Maximum palaeotemperature‡ (°C)	Onset of cooling‡ (Ma)	Maximum palaeotemperature‡ (°C)	Onset of cooling‡ (Ma)
Gane-1													
GC883-3	510–515	63–62	15	35.1 ± 3.5	93% 26	12.15 ± 0.23	1.91 67	100–115	48–22	70–85	13–2	–	–
Gro-3													
GC883-8	750–780	70–65	23	30.2 ± 4.2	0.3% 18	13.40 ± 0.25	0.66 7	>105	44–21	–	–	30–80	27–0
GC883-9	1000–1020	74–70	30	34.3 ± 7.2	<0.1% 21	12.10 ± 0.51	2.03 16	115–140	51–24	75–105	10	50–105 ⩽ 75	27–0 (4)
GC883-10	1705–1715	112–89	51	10.2 ± 2.8	0.2% 16	11.95 ± 0.58	1.92 11	160–180§	>25	125–135	22–7	65–120	7–0
GC883-11	2105–2115	112–89	63	11.4 ± 3.7	1.8% 17	12.63 ± 2.07	2.93 2	–	–	>120	20–10	<120	10–0
GC883-12	2370–2415	112–89	72	8.0 ± 2.8	5.4% 13	12.76	– 1	–	–	>120	16–8	<120	8–0
GC883-13	2760–2780	112–89	83	4.9 ± 1.8	8.5% 14	–	– 0	–	–	>115	15–8	<125	8–0
GC883-14	2965–2980	112–89	89	1.8 ± 0.9	17.2% 13	11.98 ± 0.75	1.07 2	–	–	–	–	>115	10–2
						Combined timing estimates (Ma):¶			**44–25**		**13–10**		**7–2**
						Synthesis of a larger dataset (Ma):‖			**40–30**		**11–10**		**7–2**

*Present temperature estimates based on an assumed surface temperature of 0 °C and a present-day thermal gradient of 30 °C km^{-1}.

†Central age (Galbraith & Laslett, 1993), used for samples containing a significant spread in single grain ages ($P(\chi^2)$ <5%), otherwise the 'pooled age' is quoted. All ages were calculated using the zeta calibration approach of Hurford & Green (1983) and CN5 dosimeter glass, using a zeta value of 380.4 ± 5.7 (analyst C. O'Brien), except for sample GC883-3 (zeta = 392.9 ± 7.4; analyst M. E. Moore). All errors quoted at ±1σ. All analytical details are as described by Green *et al*. (2001*b*), with the exception that the thermal neutron irradiation showed a significant flux gradient, and the appropriate value of ρ_D was determined by linear interpolation through the stack of grain mounts.

‡Thermal history interpretation of AFTA data is based on assumed heating and cooling rates of 1 °C Ma^{-1} and 10 °C Ma^{-1}, respectively (see text). Quoted ranges for palaeotemperature and onset of cooling correspond to ±95% confidence limits. Where quoted maximum palaeotemperatures represent a lower limit (e.g. <120 °C), the times quoted for the onset of cooling refer in these samples to the time at which the sample cooled through the quoted palaeotemperature.

§The maximum palaeotemperature of 160–180 °C quoted for sample GC883-10 is derived from VR data, whereas AFTA data show that cooling from these palaeotemperatures must have been prior to 25 Ma.

¶Combined timing estimates, assuming that data from all samples represent the effects of regionally synchronous cooling episodes.

‖See details of the larger dataset available in the data repository (Green 2003).

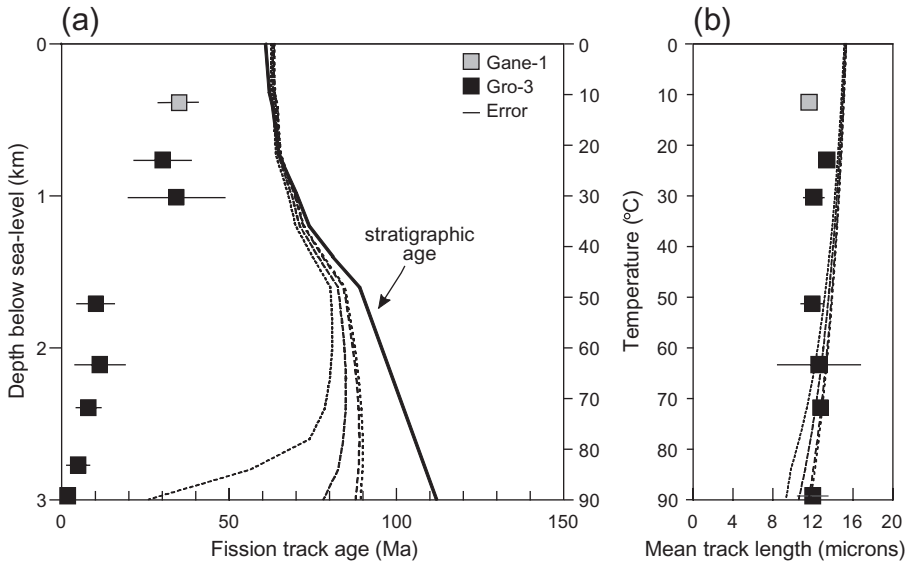

Fig. 4. (**a**) Fission-track ages and (**b**) mean track lengths in samples from the Gro-3 and Gane-1 boreholes plotted against depth and temperatures (Table 2). The continuous line in (**a**) shows the variation of stratigraphic age with depth. The dashed lines show the predicted patterns of fission-track age and mean track length from the default thermal history based on the preserved sedimentary section for apatites containing 0.0–0.1, 0.4–0.5, 0.9–1.0 and 1.5–1.6 wt% Cl. The fission-track ages decrease with depth and are much less than the values predicted from the default thermal history. This shows that the sampled sedimentary units have been much hotter in the past.

restricted to these intervals. The 'Eocene–Oligocene' episode is resolved only in the shallower samples, because deeper samples cooled to temperatures at which fission tracks are retained only from the 'Miocene' episode (from <110 to 120 °C, depending on Cl content within a particular apatite). The 'Miocene' episode is recognized in all samples except the deepest, which cooled below 115 °C only during the 'Pliocene' episode.

The consistency of the interpretations from all samples suggests that the assumption of synchronous cooling throughout the section is valid. Synthesis of a larger dataset from the Nuussuaq Basin described by Green (2003) is consistent with this assumption and allows the timing of the onset of cooling episodes to be refined further: 40–30 Ma ('Eocene–Oligocene'); 11–10 Ma ('Miocene'); 7–2 Ma ('Pliocene'). We suggest that these episodes applied to the whole region of central West Greenland.

Integration of AFTA with VR data

The palaeotemperatures obtained from the AFTA values in the Gane-1 and Gro-3 boreholes are highly consistent with the range of temperatures for the 'Eocene–Oligocene' episode derived from VR data in the shallow samples (Tables 1 and 2; Fig. 6) (see Green *et al*. 2001*a*, *b*). The deeper samples were totally annealed prior to 'Miocene' cooling, and do not record the maximum temperature 'Eocene–Oligocene' episode that determined the VR values. Two VR values from the Gane-1 well indicate relatively low palaeotemperatures, and these may reflect suppression in the reflectance of these samples (e.g. Wilkins *et al*. 1992; Newman 1997; Carr 2000).

Whereas AFTA data from sample GC883-10 reveal that the sample began to cool from a peak palaeotemperature between 125 and 135 °C between 22 and 7 Ma, VR data from a similar depth define a maximum palaeotemperature between 160 and 180 °C. This apparent conflict can be resolved if the sample that provided the AFTA data cooled from the higher palaeotemperature prior to 35 Ma (Table 2). The combination of AFTA and VR data from this sample therefore suggests three discrete episodes of cooling, and results from the other samples are consistent with this scenario.

Palaeotemperature profiles and mechanisms of heating and cooling

'Eocene–Oligocene' palaeotemperature constraints from the combined dataset define a linear profile with depth that shows consistency between the maximum palaeotemperatures derived

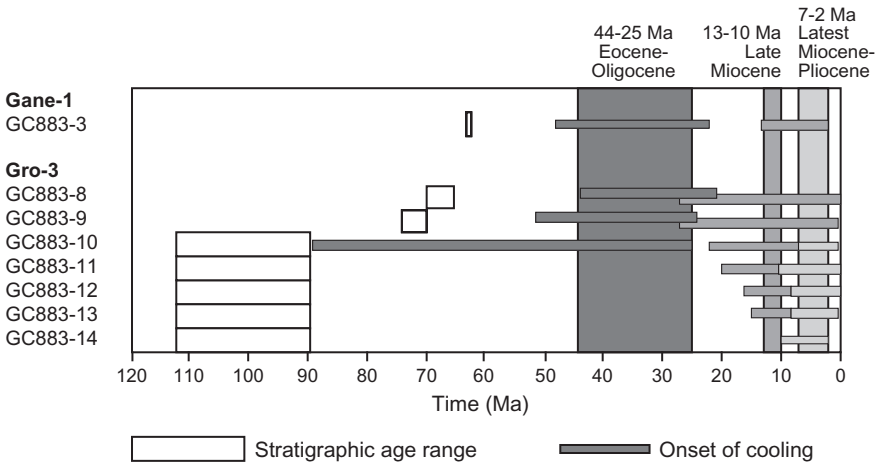

Fig. 5. Constraints on the timing of cooling in palaeothermal episodes recognized from AFTA data in the Gro-3 and Gane-1 boreholes (Table 2). Synthesis of all data suggests three discrete episodes of cooling (vertical bands). Analysis of a larger dataset from the Nuussuaq Basin allows the onset of cooling episodes to be refined further to 40–30 Ma ('Eocene–Oligocene'), 11–10 Ma ('Miocene') and 7–2 Ma ('Pliocene') (Green 2003).

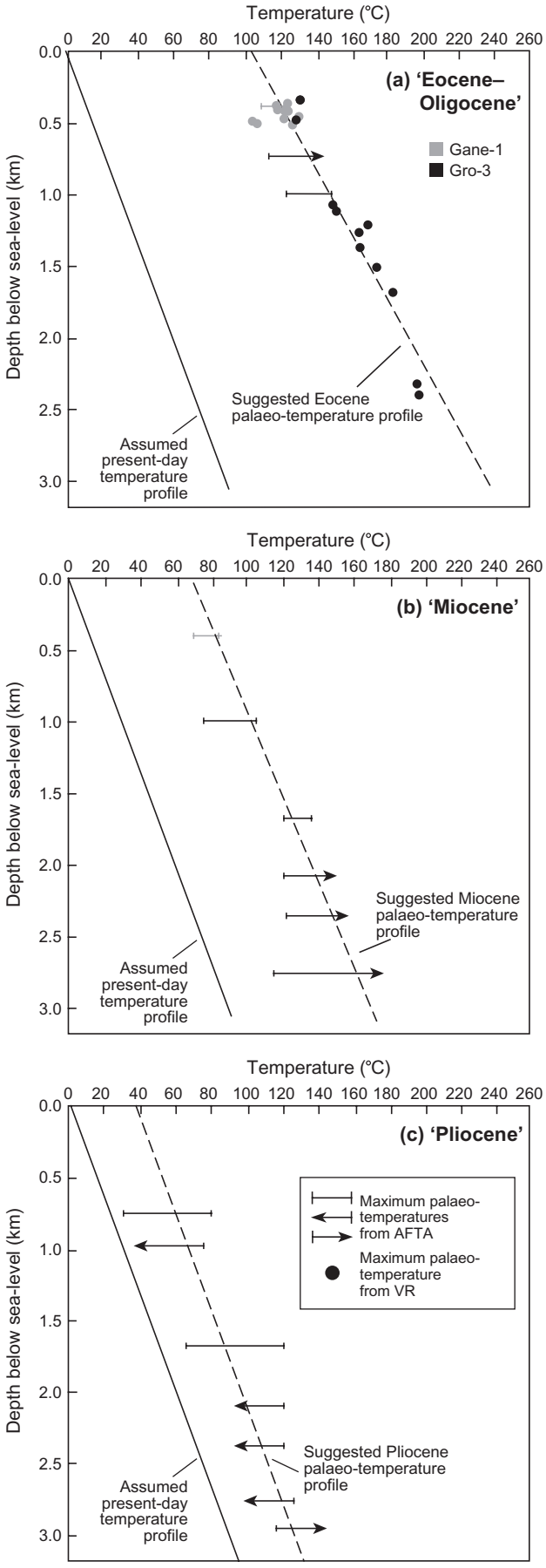

Fig. 6. Palaeotemperature constraints v. depth. Three palaeothermal episodes derived from AFTA and VR data in samples from the Gro-3 and Gane-1 boreholes. (**a**) 'Eocene–Oligocene', 40–30 Ma. (**b**) 'Miocene', 11–10 Ma. (**c**) 'Pliocene', 7–2 Ma. The present-day temperature profile is based on assuming a thermal gradient of 30 °C km^{-1}, which is in agreement with estimates from offshore wells.

from VR data and those defined from AFTA (Fig. 6a). The slope of this trend is higher than the assumed present-day temperature gradient and is offset to higher palaeotemperatures by an amount that increases from *c*. 100 °C at present-day sea level to *c*. 150 °C at a depth of 3 km. The nature of this profile suggests that the 'Eocene–Oligocene' palaeotemperatures are best explained in terms of heating as a result of a combination of deeper burial and elevated basal heat flow compared with the present-day value.

In contrast to the 'Eocene–Oligocene' values, 'Miocene' palaeotemperature constraints are rather broad in the shallower samples, whereas deeper values represent only minimum limits (owing to total annealing of all tracks prior to cooling), resulting in a less well-defined profile. 'Pliocene' constraints are also relatively broad, with only upper limits in many samples. Thus, although palaeotemperature constraints for both episodes are consistent with linear profiles, as shown in Figure 6, a range of gradients is possible for both episodes. 'Miocene' palaeotemperatures are offset to higher temperatures by around *c*. 70 °C, whereas 'Pliocene' values are higher by *c*. 40 °C, both in comparison with an assumed present-day geothermal gradient of 30 °C km^{-1}.

Because we have palaeotemperature estimates over a range of depths, we can define palaeogeothermal gradients that are consistent with the data during each episode. Extrapolation of the gradients from present-day sea level to an assumed palaeosurface temperature provides an estimate of the amount of section that formerly existed above present-day sea level at each palaeothermal maximum. Estimating how much section has been removed depends on certain assumptions, as follows.

(1) The palaeogeothermal gradient through the removed section, which cannot be constrained by direct measurement. We have assumed that the gradient was linear and equal to the value through the preserved section. This assumption may be invalid if the elevated palaeotemperatures were caused by processes such as confined fluid flow or igneous intrusion, but no evidence of such effects has been seen in the Gro-3 or Gane-1 results.

(2) The palaeosurface temperatures, which we have assumed to be 20 °C, 10 °C and 0 °C, respectively, for the 'Eocene–Oligocene', 'Miocene' and 'Pliocene' episodes. These values are based on mollusc shell isotope data for the North Sea reported by Buchardt (1978), but are also considered reasonable for the study area.

The calculated palaeotemperatures for each episode can be explained by different combinations of palaeothermal gradients and amounts of removed section, with higher palaeothermal gradients requiring less removed section and vice versa, as shown in Figure 7 (Bray *et al*. 1992; Green *et al*. 1995, 2002).

(1) The 'Eocene–Oligocene' episode is well defined by coherent data over a depth range of *c*. 2.5 km and is characterized by a palaeogeothermal gradient between 40 and 48 °C km^{-1} (Fig. 6a). This corresponds to an overburden of 1500–2000 m above present-day sea level when cooling began between 40 and 30 Ma.

(2) The 'Miocene' palaeotemperatures allow a much wider

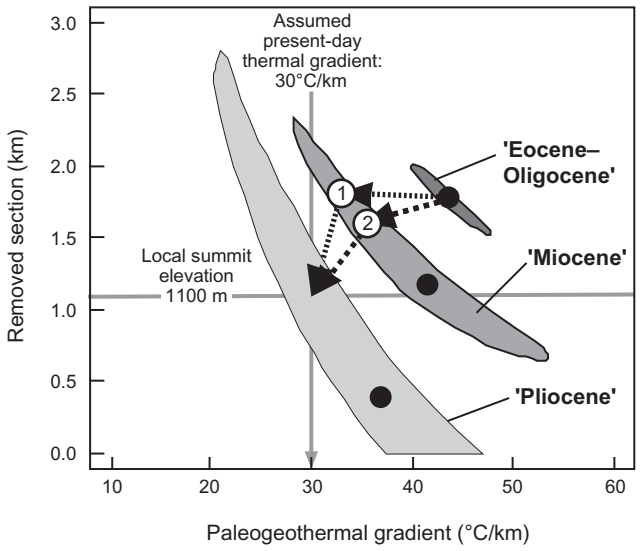

Fig. 7. Amounts of additional section and palaeogeothermal gradients required to explain palaeothermal episodes in the composite Gro-3 and Gane-1 borehole dataset. The wells were sited near the mouth of a steep-sided valley with flanking summits reaching elevations of *c*. 1100 m in Palaeocene volcanic rocks. Thus a succession of volcanic rocks of at least this thickness must once have covered the present-day ground surface. The shaded regions define the parameter ranges that are consistent with the respective palaeotemperature constraints within 95% confidence limits. Trajectories labelled 1 and 2 refer to the burial-uplift histories illustrated in Figures 8 and 9. ●, maximum likelihood solutions.

range of possible palaeogeothermal gradient from 28 to 53 °C km^{-1}. This corresponds to an overburden of 700–2300 m above present-day sea level when cooling from this palaeotemperature peak began between 11 and 10 Ma.

(3) The 'Pliocene' palaeotemperatures can be explained by a palaeothermal gradient between 20 and 48 °C km^{-1}. This corresponds to an overburden of between 0 and 3 km above present-day sea level when cooling began between 7 and 2 Ma.

Constraints from present-day topography

The present-day topography imposes a significant constraint on the amount of section that can have been present above the surface at the site of each borehole. Both were sited near the mouth of a steep-sided valley with flanking summits reaching elevations of *c*. 1100 m in Palaeocene volcanic rocks. Thus a succession of volcanic rocks of at least this thickness must once have covered the present-day ground surface.

(1) 'Pliocene' episode. The range of conditions that characterize the 'Pliocene' episode intersects the 1100 m summit elevation at a palaeogeothermal gradient of 30 °C km^{-1} (Fig. 7). This means that the 'Pliocene' palaeotemperature constraints can be explained by a combination of a surface temperature of 0 °C, a palaeogeothermal gradient equal to the (assumed) present-day value and burial by exactly the amount of section that was eroded in creating the present-day local relief. We therefore interpret that the cooling during the 'Pliocene' episode corresponds to incision of the local relief, which can therefore be dated to have begun between 7 and 2 Ma.

(2) 'Eocene–Oligocene' episode. In contrast, the range of conditions that characterizes the 'Eocene–Oligocene' episode in Figure 7 plots entirely above the local summit elevation of 1100 m. This observation indicates that the present-day adjacent summits were more deeply buried by 400–900 m at the time that cooling began, with the appropriate amount depending on what value of palaeogeothermal gradient is chosen from the allowed range of 40–48 °C km^{-1}.

(3) 'Miocene' episode. The 'Miocene' palaeotemperature constraints allow a wide range of palaeogeothermal gradients and additional burial (Fig. 7): At one extreme, palaeogeothermal gradients around 40–45 °C km^{-1} (Fig. 7) correspond to *c*. 1100 m of section above present-day sea level, implying that the adjacent summit level was no more deeply buried during the late Miocene than at the present day. In this case, 'Miocene' cooling was due solely to a reduction in the palaeogeothermal gradient, and erosion did not begin until the start of incision of the present-day relief in the 'Pliocene' episode. At the other extreme, a palaeogeothermal gradient of *c*. 30 °C km^{-1} (Fig. 7) corresponds to a total section of *c*. 2000 m above present sea level, implying that the adjacent summit level was buried by an additional *c*. 900 m. In this case, 'Miocene' cooling was due solely to erosion of the overburden without change in geothermal gradient and began between 11 and 10 Ma.

A variety of alternative scenarios could also be constructed that would be consistent with the available palaeotemperature constraints, and further geological input is required before a choice can be made between them. Most volcanism in the area took place during the Palaeocene, followed by a second episode during the early Eocene, after which comparatively minor volcanic activity took place (Storey *et al*. 1998). It seems, therefore, most likely that the palaeogeothermal gradient declined after the 'Eocene–Oligocene' episode and that some erosion did take place during the 'Miocene' episode. Consequently, the start of erosion at that time probably implies the start of the Neogene uplift in the area. The upper limit of *c*. 900 m for the amount of additional 'Eocene–Oligocene' burial of the adjacent summit level is the same as that for the 'Miocene' episode. Therefore it remains unclear whether 'Eocene–Oligocene' cooling involved erosion of the overburden or was due solely to reduction in heat flow and a drop in surface temperature.

Reconstructions of the thermal and burial history

We present two possible reconstructions of the thermal and burial–erosion history that are consistent with the constraints derived from AFTA and VR data from the Gro-3 and Gane-1 boreholes (Figs. 8 and 9). In undertaking such reconstructions, it is important to take note of what can and what cannot be constrained using palaeothermal techniques such as AFTA and VR. As emphasized by Green *et al*. (2002), such techniques are dominated by palaeotemperature maxima, but retain no information on the history prior to the onset of cooling. In a sedimentary section that has undergone multiple heating and cooling episodes, as in this study, the data cannot constrain the history between cooling events, although the magnitude and timing of the palaeothermal peaks are well defined. The precise details of the history prior to the onset of 'Eocene–Oligocene' cooling is therefore unconstrained by the AFTA and VR data and that shown here is based, in part, on the subsidence known to have taken place during the Palaeocene.

The reconstruction of the maximum palaeotemperature episode ('Eocene–Oligocene') is tightly constrained by the data, so both reconstructions are represented by (1) 1100 m of additional burial between 61 and 60 Ma (representing the effects of the

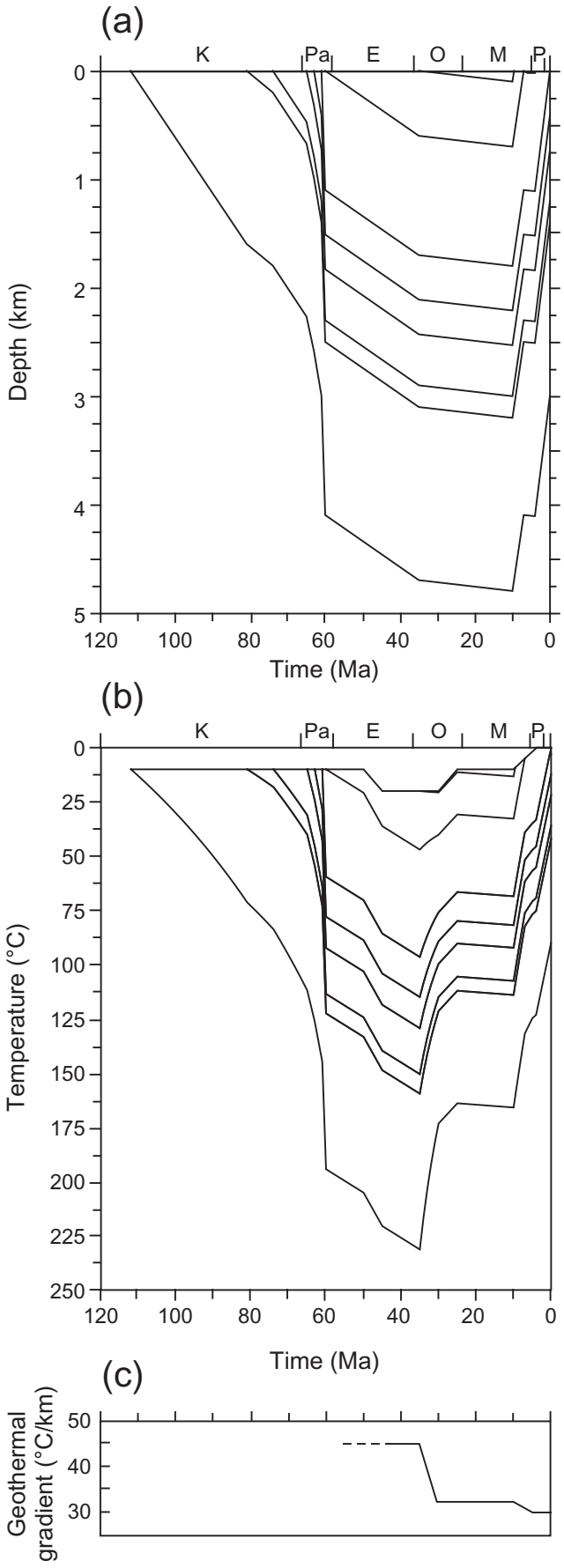

volcanic succession preserved in neighbouring peaks), and (2) a further 600 m of burial between 60 and 40 Ma, giving (3) a total additional burial of 1700 m at 40 Ma, with a palaeogeothermal gradient at that time of 45 °C km^{-1} (see Fig. 7). This model is consistent with the known geology of the Nuussuaq Basin combined with a hypothesized episode of thermal subsidence and infilling of post-volcanic rocks.

The nature of the 'Pliocene' episode is also common to both reconstructions, representing the incision of the modern relief (1100 m), modelled to have taken place since 4 Ma, although an onset at any time between 7 and 2 Ma is allowed by the AFTA data.

Many alternatives satisfy the data for the 'Miocene' episode (Fig. 7) and two possible reconstructions are shown in Figures 8 and 9. Figure 8 shows continued burial through Eocene and Oligocene times, with maximum burial depths reached in the late Miocene (compare the trajectory labelled '1' in Fig. 7). Figure 9 incorporates an episode of Eocene–Oligocene exhumation and Miocene reburial (trajectory '2' in Fig. 7). Further integration with geological constraints is required before discrimination between the various options is possible.

Summary of constraints imposed by AFTA and VR data

Palaeogeothermal gradients and palaeoburial estimates are based on data from the Gro-3 and Gane-1 wells, whereas the timing of the episodes of onset of cooling is based on a larger dataset from the Nuussuaq Basin, the details of which have been described by Green (2003). The main constraints imposed by the AFTA and VR data are as follows.

(1) The section intersected in the two boreholes began to cool from maximum post-depositional palaeotemperatures sometime between 40 and 30 Ma ('Eocene–Oligocene' cooling episode).

(2) At the time that this cooling episode began, the sampled section was buried by an additional 400–900 m of section above the level of the adjacent summits (1500–2000 m deeper burial than at the present day), and the palaeogeothermal gradient was between 40 and 48 °C km^{-1} (Fig. 7).

(3) Subsequent cooling from lower palaeothermal peaks began between 11 and 10 Ma and between 7 and 2 Ma ('Miocene' and 'Pliocene' cooling episodes).

(4) Available palaeotemperature constraints allow a wide range of values of palaeogeothermal gradient and additional burial during the 'Miocene' episode (Fig. 7).

Fig. 8. Burial and thermal history reconstruction 1 for the Gro-3 well (see Fig. 7). (**a**) Depth v. time; (**b**) temperature v. time with palaeosurface temperatures indicated by the upper line; (**c**) palaeogeothermal gradient v. time. In this reconstruction the 'Eocene–Oligocene' cooling episode is due entirely to reduction in palaeogeothermal gradient and fall in surface temperature. The maximum palaeotemperature episode ('Eocene–Oligocene') is represented by 1100 m of additional burial between 61 and 60 Ma (representing the effects of the volcanic succession preserved in neighbouring peaks) and a further 600 m of burial between 60 and 40 Ma, giving a total additional burial of 1700 m at 40 Ma. This was followed by deposition of an additional 100 m until late Miocene time, resulting in maximum depth of burial at 10 Ma, after which exhumation commenced. Between 10 and 7 Ma, 700 m of erosion occurred and, after a period of relative quiescence, the remaining 1100 m were removed during the 'Pliocene' episode. The erosion prior to volcanism is not shown because it is not recorded in the thermochronological data. A late Miocene palaeogeothermal gradient of 32.5 °C km^{-1} has been used. Palaeosurface temperatures are based on Buchardt (1978). K, Cretaceous; Pa, Palaeocene; E, Eocene; O, Oligocene; M, Miocene; P, Pliocene.

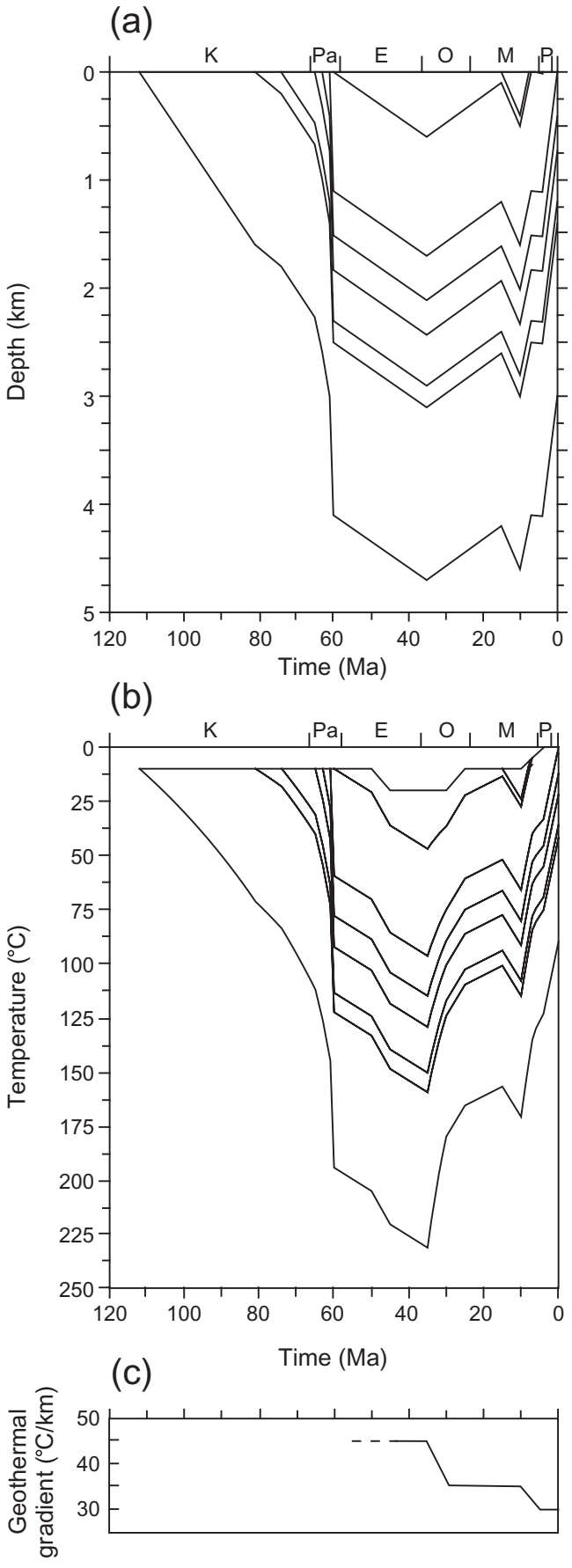

(5) The most recent cooling episode, beginning sometime between 7 and 2 Ma, corresponds to incision of the present-day relief (*c*. 1100 m) below the adjacent summit level, corresponding to a geothermal gradient of 30 °C km^{-1}, which is in agreement with estimates from offshore wells.

Although incision of the valleys since the inception of the most recent uplift at 7–2 Ma will have produced a local perturbation of the isotherms, this does not affect our interpretation because the AFTA data record the pre-incision palaeothermal state, in which the isotherms would have been parallel to the (assumed) flat land surface.

Comparison with previous studies

Bojesen-Koefoed *et al*. (1997) concluded that a section 1900 m thick must have been present above the present-day ground surface at the location of the Gro-3 well prior to erosion, to produce the observed maturity trend in the well (Fig. 6a). The estimate was made by extrapolating the VR depth trend linearly to a VR value of 0.2. The estimate of Bojesen-Koefoed *et al*. (1997) agrees well with the 1500–2000 m found by this study as the most probable value for the missing section.

Mathiesen (1998) used a basin modelling approach constrained by thermal maturation data and apatite fission-track data to define consistent models of burial, uplift and erosion for the Nuussuaq Basin. The VR data available to Mathiesen (1998) were those used in this study, but the fission-track data available to him were from an earlier study and were too limited to achieve a well-defined timing of uplift and erosion. His preferred models for the Gro-3 well did, however, indicate accelerated erosion during the Neogene, whereas uncertainty in determining the palaeogeothermal gradient led to estimates of the missing section ranging from 2050 to 3350 m. The low value was supported by the maturity data from the Gro-3 well, whereas the high value was based on extrapolation of the top basalt surface offshore reported by Chalmers (2000).

Chalmers (2000) showed that a >3 km thick, post-mid-Eocene sedimentary section offshore west of Nuussuaq had been rotated to dip westwards and its landward end is truncated either by an erosional unconformity close to the sea bed or by the sea bed itself. Chalmers (2000) concluded that rotation of the section, and thus uplift of the landmass on Nuussuaq, had occurred substantially after the mid-Eocene and probably during the

Fig. 9. Burial and thermal history reconstruction 2 for the Gro-3 well (see Fig. 7). (**a**) Depth v. time. (**b**) Temperature v. time with palaeosurface temperatures indicated by the upper line. (**c**) Palaeogeothermal gradient v. time. In this reconstruction the 'Eocene–Oligocene' cooling episode involves exhumation. The burial history between 61 and 40 Ma is the same as in reconstruction 1 (Fig. 8). In this reconstruction 500 m of section was removed during a discrete phase of exhumation between 35 and 15 Ma, following which an additional 400 m of section was deposited between 15 and 10 Ma, giving a total thickness of additional burial ('palaeoburial') at that time of 1600 m. Erosion of 500 m of section occurred between 10 and 7 Ma and the remaining sediments were removed as in reconstruction 1. The erosion prior to volcanism is not shown because it is not recorded in the thermochronological data. A late Miocene palaeogeothermal gradient of 35 °C km^{-1} has been used in this reconstruction. Palaeosurface temperatures are based on Buchardt (1978). K, Cretaceous; Pa, Palaeocene; E, Eocene; O, Oligocene; M, Miocene; P, Pliocene.

Neogene. The extrapolation by Chalmers (2000) included estimates of the amount of post-basalt movement across two faults and resulted in an estimate of a palaeobasalt surface at 3350 m above the present-day site of Gro-3.

The analysis presented here clearly shows the consistency of AFTA and VR data from the Gro-3 and Gane-1 wells and thus favours the minimum erosion case of Mathiesen (1998) based on a high'Eocene–Oligocene' palaeogeothermal gradient (Fig. 6a). The refutation of the maximum erosion case implies that either a major part of the fault movements must have taken place after maximum temperatures occurred during the 'Eocene–Oligocene' episode or that the estimates of Chalmers (2000) of the amount of displacement across the faults are wrong.

Discussion

It is interesting that we find that maximum palaeotemperatures in the subsurface occurred between 40 and 30 Ma, which is significantly later than peak volcanism during the Palaeocene. In addition, the erosion prior to volcanism, well documented by Dam & Sønderholm (1998) and Dam *et al*. (1998), is not recorded in the thermochronological data because it happened prior to the palaeotemperature maximum. If the geothermal gradient is assumed to have declined after peak volcanism in the Palaeocene, the 'Eocene–Oligocene' palaeotemperature maximum must represent continued burial of the sedimentary succession prior to the 'Eocene–Oligocene' episode. This conclusion agrees with the known stratigraphic record, because Eocene volcanic rocks are present further west on Nuussuaq (Storey *et al*. 1998) and Eocene sedimentation is documented just west of Nuussuaq. Here a seismic unit between the top basalt and the mid-Eocene reflector is seen on seismic sections (*c*. 150 ms two-way time thickness; see fig. 4 of Chalmers 2000). The mid-Eocene unconformity is represented by a hiatus in the offshore stratigraphic record in the Lutetian, *c*. 45–43 Ma (Eldrett *et al*. 1996; Nøhr-Hansen 2003). Sediments of late Eocene age (older than 34 Ma) are found in the wells offshore southern West Greenland, whereas sediments of Oligocene age have not been identified (Nøhr-Hansen 2003). This means that sediments older than 45 Ma and probably also between 45 and 34 Ma old sediments are preserved just west of Nuussuaq, in agreement with the suggested continued burial at the location of the two boreholes until sometime between 40 and 30 Ma.

It is not clear whether the 'Eocene–Oligocene' cooling involved erosion of the overburden or if it was due solely to reduction in heat flow and a drop in surface temperature (Figs. 8 and 9). Even though the temporal constraints are loose, this episode probably correlates with the Oligocene hiatus identified offshore southern West Greenland (Nøhr-Hansen 2003; Piasecki 2003). The Oligocene hiatus does not appear as a prominent angular unconformity on seismic sections from the area and consequently seems not to have involved significant tectonism. If it represents uplift and erosion, the uplift must have been uniform over a very large area, but the hiatus may well represent only non-deposition. If the 'Eocene–Oligocene' episode involved erosion, then reburial must have taken place to attain the Miocene burial depths required by the AFTA data as shown in reconstruction 2 in Figure 9. Indication of such a phase of sedimentation may be present on Hareøen, where a succession of Neogene sediments has been found in a palaeofumarole (Christiansen *et al*. 1999).

The nature of the 'Miocene' cooling episode can be understood if the palaeotemperature constraints allowed by AFTA and VR data are narrowed by geological arguments. Because there was only minor volcanism after early Eocene times, the geothermal gradient probably declined to its present value after the palaeothermal event between 40 and 30 Ma. Consequently, the 'Miocene' cooling episode must partly have been due to erosion, which is implicit in both reconstructions shown in Figures 8 and 9. A scenario of no erosion in this episode requires that the palaeogeothermal gradient was as high as the gradient during the 'Eocene' episode, 40–45 °C km^{-1} (Fig. 7). Therefore, if the gradient was less than that, there must have been some erosion since 10 Ma.

The episodes of cooling during the Cenozoic identified in this study agree well with episodes in NE Greenland beginning between 40 and 30 Ma and between 10 and 5 Ma found in a similar study of AFTA data from outcrop samples (Thomson *et al*. 1999*a*). In this area maximum palaeotemperatures were also found to have occurred during the mid-Cenozoic corresponding to an additional palaeoburial of up to 3 km if a geothermal gradient of 30 °C km^{-1} is assumed (Thomson *et al*. 1999*a*). The coincidence in timing between the mid-Cenozoic episodes identified on the west and east coast of Greenland suggests that they may have a common cause, and that this is related either to uplift and erosion or only to reduction in heat flow and a drop in surface temperature. Only minor occurrences of mid-Cenozoic magmatic intrusions are known from West Greenland (e.g. Storey *et al*. 1998), so it is unlikely that heat from such intrusions could be the cause of the palaeothermal episode between 40 and 30 Ma as suggested by Thomson *et al*. (1999*a*) for their study area in NE Greenland.

The Neogene event identified on the east coast may represent the combined effect of the two events identified on the west coast. Thomson *et al*. (1999*a*) suggested that the late event was related to uplift and erosion and that the event resulted from changes in the North Atlantic spreading direction. The results presented here suggest that it is likely that the event on the east coast is indeed due to uplift and erosion, as on the west coast, whereas changing plate movements in the North Atlantic are a less likely cause on the west coast of Greenland and so by analogy not on the east coast either. Other studies from East Greenland based on analysis of apatite fission tracks have also concluded that kilometre-scale erosion took place during the Neogene (Johnson & Gallagher 2000; Mathiesen *et al*. 2000; Hansen & Brooks 2002).

Estimates of the magnitude of the Neogene uplift in West Greenland are constrained by the occurrence of marine Palaeocene deposits within the basalt succession at *c*. 1200 m a.s.l. (Piasecki *et al*. 1992). Indeed, these basalts may be considered as the cap rock that has prevented the underlying sedimentary succession from being completely removed. It is thus only due to the kilometre-scale Neogene uplift and dissection within the last 11 Ma that the Mesozoic–Palaeogene succession of the Nuussuaq Basin has been re-exposed and that we are able to study the effects of the impact of the Iceland plume on these sediments.

Exhumation in West Greenland was also affected by glacial erosion during the late Cenozoic. The first indications of late Cenozoic glaciation have been found in cores of late Miocene age collected offshore southern East Greenland (Larsen *et al*. 1994). The episode of uplift and erosion reported in this paper that began between 11 and 10 Ma thus clearly precedes glaciation in Greenland. Isostatic rebound after the last glaciation is clearly too small to explain the magnitude of erosion in the study area, where the altitude of the post-glacial marine limit is less than 120 m a.s.l. (Funder & Hansen 1996).

Possible causes of Neogene uplift

The causes of Neogene uplift in West Greenland (and around the northern North Atlantic) are as yet unknown, but our observations can be used to rule out some of the proposed mechanisms. Uplift during the Palaeocene and/or early Eocene was a common phenomenon around the northern North Atlantic, and has been attributed to dynamic support during impact of the Iceland plume and permanent underplating afterwards (e.g. Jones *et al*. 2002, and references therein). Uplift and erosion of the northern British Isles was the source of a rapid sediment influx into, for example, the Viking and Faeroe–Shetland Basins at this time. The contemporaneous basalts exposed west of Scotland were all erupted onto major unconformity surfaces, although Bell & Williamson (2002) considered that the unconformities may be local and attributed them 'to the initial stages of growth of the central complexes'. Many workers (e.g. Jones *et al*. 2002) consider that this uplift was permanent, as a result of underplating, and that this event lifted present-day mountain areas in the region. Our observation that rapid subsidence to well below sea level followed this uplift phase and that the uplift to present-day heights took place much later seems to rule out that argument. Comparable Palaeogene subsidence took place west of Scotland, where a substantial proportion of the Palaeogene lavas offshore are deeply buried by Eocene–Recent sediments (Bell & Williamson 2002). That Palaeogene lavas crop out west of Scotland and on the Faeroe Islands is probably because of late Cenozoic uplift in these areas as is the case in West Greenland (e.g. Japsen 1997, 1998; Thomson *et al*. 1999*b*; Green *et al*. 2001*b*; Andersen *et al*. 2002; Stoker 2002; Stoker *et al*. 2005).

The uplift during the Palaeogene was probably caused by dynamic support during plume impact combined with space problems as plume material travelled laterally at the base of the lithosphere. The subsequent rapid subsidence may partly be due to the withdrawal of dynamic support as ascent of the plume head slowed, and partly to withdrawal of magma from crustal or upper-mantle magma chambers as eruption proceeded. Whether these mechanisms are enough to explain all the subsidence will require quantitative modelling beyond the scope of this paper.

Intraplate compressional stresses resulting from 'ridge push' have been suggested by some workers (e.g. Doré *et al*. 1999) to explain the Neogene uplift of Scandinavia. As Chalmers (2000) pointed out, sea-floor spreading ceased in the Labrador Sea during the Eocene at around 40 Ma (Srivastava & Keen 1995), whereas, as we have shown here, significant uplift in West Greenland took place only after *c*. 10 Ma.

Scarp retreat of an uplifted rift flank has been suggested as the driving force behind the denudation history of northern Scandinavia (Hendriks & Andriessen 2002). This mechanism may have caused the Maastrichtian uplift and channel erosion on Nuussuaq (Dam *et al*. 1998), but is clearly not applicable to the Neogene phases in West Greenland, where the last phase of rifting occurred *c*. 50 Ma earlier (Chalmers & Pulvertaft 2001). There is, however, no doubt that some component of the Neogene uplift of the present-day mountain tops must be due to isostatic compensation for erosion. Riis & Fjeldskaar (1992) estimated that approximately two-thirds of the uplift of northern Scandinavia was due to isostacy, and Rohrman *et al*. (2002) calculated that approximately one-third of southern Scandinavia's uplift can be attributed to this effect. No calculations have been carried out for western Greenland.

Other mechanisms are consistent with our observations, although perhaps not entirely in the form originally proposed by their authors. Tectonic forces must have been involved in producing the Neogene kilometre-scale east–west tilting of the Palaeogene basalts in West Greenland as well as the late Cenozoic normal faulting inferred from a recent study of large landforms (Bonow 2004). Such a tectonic component may be reinforced by an isostatic response to erosional removal of material, but a mechanism is needed to trigger the erosion and it appears that this mechanism must be deep rooted.

Variations in flux from the plume that caused instabilities where the crust or lithosphere changes rapidly in thickness seem one possible cause (Stuevold & Eldholm 1996). Nielsen *et al*. (2002) and Rohrman *et al*. (2002) have suggested that a Rayleigh–Taylor instability may have formed where hot plume asthenosphere met cooler subcontinental asthenosphere (Rohrman *et al*. 2002) or where horizontally travelling plume material eroded the base of the lithosphere where lithosphere thickness changed rapidly (Nielsen *et al*. 2002). Uplift would result from resultant mantle upwelling or asthenospheric diapirism (Rohrman & van der Beek 1996). This mechanism also offers an explanation for anomalous basin subsidence where asthenospheric material flowed from below the basin toward the upwelling; that is, that the late Cenozoic uplift of West Greenland, Scandinavia and the British Isles is concurrent with subsidence and sedimentation offshore (see Japsen & Chalmers 2000). However, the proposal of Nielsen *et al*. (2002) that the Rayleigh–Taylor instability formed during the Palaeogene impact of the plume and that subsequent uplift is isostatic does seem to be ruled out. One or more events during the Neogene are necessary.

Conclusions

Several episodes of uplift, erosion and subsidence during the Cenozoic have been identified on Nuussuaq, as follows.

(1) Uplift as a result of the impact of the Iceland plume in the early Palaeocene resulted in valley incision that was followed by rapid subsidence and transgression. Subsidence continued so that water depths were *c*. 700 m during early volcanism and even later subsidence kept pace with aggradation of the lava pile to a total thickness of over 1 km.

(2) Uplift and erosion took place in two phases during the Neogene, one starting in the late Miocene between 11 and 10 Ma and the other in the latest Miocene–Pliocene between 7 and 2 Ma. Assuming a present-day geothermal gradient of 30 °C km^{-1}, a section of *c*. 1100 m was removed during the latest episode from above the locations of the Gro-3 and Gane-1 wells corresponding to incision of the relief below the adjacent summit level. The section removed during the late Miocene episode cannot be estimated accurately because of uncertainty about the geothermal gradient during that period. We conclude that most of the present-day relief on Nuussuaq, with summits up to 2100 m a.s.l., was formed by erosion of rocks that were uplifted during the two Neogene phases.

(3) An intermediate episode, involving cooling of rocks in the subsurface, began during the mid-Cenozoic (40–30 Ma), but thermochronological data alone are insufficient to determine whether this cooling definitely involved erosion of the overburden or if it was due solely to reduction in heat flow and a drop in surface temperature. Maximum palaeotemperatures occurred at this time and, based on an estimated palaeogeothermal gradient of 40–48 °C km^{-1}, since then a total section of *c*. 1500–2000 m has been removed from above the location of the wells.

We conclude that uplift from the effects of the Iceland plume in West Greenland during the Palaeogene was transient and was

quickly followed by kilometre-scale subsidence. Analysis of apatite fission-track and vitrinite-reflectance data shows that the present high mountains in central West Greenland are erosional remnants from uplift events that occurred during the Neogene. More detailed understanding of the lateral variations of the present relief in relation to uplift and erosion and of the nature of the mid-Cenozoic event requires detailed analysis of large-scale landforms and additional AFTA and VR data.

We have demonstrated the existence of two Cenozoic uplift phases that are clearly separated in time by as much as 50 Ma and by their completely different nature. Elsewhere around the North Atlantic where Mesozoic and Palaeogene rocks crop out, such exhumation has often been attributed to late Cenozoic uplift and erosion (see references given by Japsen & Chalmers (2000) and Doré *et al*. (2002)). However, these areas comprise regions that were also affected by the Iceland plume during the Palaeogene (e.g. East Greenland, the northern part of the British Isles and the Faeroe Islands) as well as regions that were unaffected by it (e.g. the southeastern part of the British Isles and southern Scandinavia). These regional differences and the observations from Nuussuaq presented here clearly demonstrate that the Neogene uplift around the North Atlantic is of a completely different nature from the uplift and subsidence that was induced by the Iceland plume during the Palaeogene.

The authors thank the Bureau of Minerals and Petroleum (Government of Greenland) for co-operation and financial support. We thank A. Mathiesen for fruitful discussions and C. Pulvertaft for his helpful comments on the manuscript. J. Bonow contributed to Figures 2 and 3. The digital elevation model is used by courtesy of KMS, Copenhagen. The paper is published with permission of the Geological Survey of Denmark and Greenland.

Note added in proof

After the completion of the paper, additonal VR data from the Gro-3 well were made available to the authors, but these affect the results only slightly. When the first cooling began, the samples from the Gro-3 and Gane-1 boreholes were buried 1750–100 m deeper than at present, and the palaeogeothermal gradient was 39–44°C km^{-1}.

References

Andersen, M.S., Sørensen, A.B., Boldreel, L.O. & Nielsen, T. 2002. Cenozoic evolution of the Faeroe Platform: comparing denudation and deposition. *In:* Doré, A.G., Cartwright, J.A., Stoker, M.S., Turner, J.P. & White, N. (eds) *Exhumation of the North Atlantic Margin: Timing, Mechanisms and Implications for Petroleum Exploration*. Geological Society, London, Special Publications, **196**, 291–311.

Aram, R.B. 1999. West Greenland versus Vøring Basin: comparison of two deepwater frontier plays. *In:* Fleet, A.J. & Boldy, S.A.R. (eds) *Petroleum Geology of Northwest Europe: Proceedings of the 5th Conference*. Geological Society, London, 315–324.

Argent, J.D., Stewart, S.A., Green, P.F. & Underhill, J.R. 2002. Heterogeneous exhumation in the Inner Moray Firth, UK North Sea: constraints from new AFTA® and seismic data. *Journal of the Geological Society, London*, **159**, 715–729.

Bell, B.R. & Williamson, I.T. 2002. Tertiary igneous activity. *In:* Trewin, N.H. (ed.) *The Geology of Scotland*. Geological Society, London, 371–407.

Berggren, W.A., Kent, D.V., Swisher, C.C. III & Aubry, M.-P. 1995. A revised Cenozoic geochronology and chronostratigraphy. *In:* Berggren, W.A., Kent, D.V., Aubry, M.-P. & Hardenbol, J. (eds) *Geochronology, Time Scales and Global Stratigraphic Correlation*. Society of Economic Paleontologists and Mineralogists, Special Publications, **54**, 129–212.

Bojesen-Koefoed, J., Christiansen, F.G., Nytoft, H.P. & Dalhoff, F. 1997. *Organic geochemistry and thermal maturity of sediments in the Gro-3 well, Nuussuaq, West Greenland*. Danmarks og Grønlands Geologiske Undersøgelse Rapport, **1997/143**.

Bonow, J. M. 2004. *Palaeosurfaces and palaeovalleys on North Atlantic previously glaciated passive margins—references for conclusions on uplift and erosion*. PhD thesis, Stockholm University.

Bray, R.J., Green, P.F. & Duddy, I.R. 1992. Thermal history reconstruction using apatite fission track analysis and vitrinite reflectance: a case study from the UK East Midlands and the Southern North Sea. *In:* Hardman, R.F.P. (ed.) *Exploration Britain: Into the Next Decade*. Geological Society, London, Special Publications, **67**, 3–25.

Buchardt, B. 1978. Oxygen isotope paleotemperatures from the Tertiary period in the North Sea area. *Nature*, **275**, 121–123.

Burnham, A.K. & Sweeney, J.J. 1989. A chemical kinetic model of vitrinite reflectance maturation. *Geochimica et Cosmochimica Acta*, **53**, 2649–2657.

Carr, A. 2000. Suppression and retardation of vitrinite reflectance, Part 1. Formation and significance for hydrocarbon generation. *Journal of Petroleum Geology*, **23**, 313–343.

Chalmers, J.A. 2000. Offshore evidence for Neogene uplift in central West Greenland. *Global and Planetary Change*, **24**, 311–318.

Chalmers, J.A. & Pulvertaft, T.C.R. 2001. Development of the continental margins of the Labrador Sea: a review. *In:* Wilson, R.C.L., Whitmarsh, R.B., Taylor, B. & Froitzheim, N. (eds) *Non-volcanic Rifting of Continental Margins: a Comparison of Evidence from Land and Sea*. Geological Society, London, Special Publications, **187**, 77–105.

Chalmers, J.A., Pulvertaft, T.C.R., Marcussen, C. & Pedersen, A.K. 1999. New insight into the structure of the Nuussuaq Basin, central West Greenland. *Marine and Petroleum Geology*, **16**, 197–224.

Christiansen, F.G., Bate, K.J., Dam, G., Marcussen, C. & Pulvertaft, T.C.R. 1996a. Continued geophysical and petroleum geological activities in West Greenland in 1995 and the start of onshore exploration. *Bulletin Grønlands Geologiske Undersøgelse*, **172**, 15–21.

Christiansen, F.G., Bojesen-Koefoed, J., Nytoft, H.P. & Laier, T. 1996b. *Organic geochemistry of sediments, oils and gases in the GANE#1, GANT#1 and GANK#1 wells, Nuussuaq, West Greenland*. Danmarks og Grønlands Geologiske Undersøgelse Rapport, **1996/23**.

Christiansen, F.G., Boesen, A. & Bojesen-Koefoed, J. *et al*. 1999. Petroleum geological activities in West Greenland in 1998. *Geology of Greenland Survey Bulletin*, **183**, 46–56.

Christiansen, F.G., Bojesen-Koefoed, J.A. & Chalmers, J.A. *et al*. 2001. Petroleum geological activities in West Greenland in 2000. *Geology of Greenland Survey Bulletin*, **189**, 24–33.

Clarke, D.B. & Pedersen, A.K. 1976. Tertiary volcanic province of West Greenland. *In:* Escher, A. & Watt, W.S. (eds) *Geology of Greenland*. Geological Survey of Greenland, Copenhagen, 365–385.

Crowhurst, P.V., Green, P.F. & Kamp, P.J.J. 2002. Appraisal of (U–Th)/He apatite thermochronology as a thermal history tool for hydrocarbon exploration: an example from the Taranaki Basin, New Zealand. *AAPG Bulletin*, **86**, 1801–1819.

Dalhoff, F., Chalmers, J.A., Gregersen, U., Nøhr-Hansen, H., Rasmussen, J.A. & Sheldon, E. 2003. Mapping and facies analysis of Paleocene–Mid-Eocene seismic sequences, offshore southern West Greenland. *Marine and Petroleum Geology*, **20**, 935–986.

Dam, G. 2002. Sedimentology of magmatically and structurally controlled outburst valleys along rifted volcanic margins: examples from the Nuussuaq Basin, West Greenland. *Sedimentology*, **49**, 505–532.

Dam, G. & Nøhr-Hansen, H. 2001. Mantle plumes and sequence stratigraphy; Late Maastrichtian–Early Paleocene of West Greenland. *Bulletin of the Geological Society of Denmark*, **48**, 189–207.

Dam, G. & Sønderholm, M. 1998. Sedimentological evolution of a fault-controlled early Paleocene incised-valley system, Nuussuaq Basin, West Greenland. *In:* Shanly, K.-W.. & McCabe, P.J. (eds) *Relative Role of Eustasy, Climate and Tectonism in Continental Rocks*. Society of Economic Paleontologists and Mineralogists, Special Publications, **59**, 109–121.

Dam, G., Larsen, M. & Sønderholm, M. 1998. Sedimentary response to mantle plumes: implications from Paleocene onshore successions, West and East Greenland. *Geology*, **26**, 207–210.

Doré, A.G., Lundin, E.R., Jensen, L.N., Birkeland, Ø., Eliassen, P.E. & Fichler, C. 1999. Principal tectonic events in the evolution of the northwest European Atlantic margin. *In:* Fleet, A.J. & Boldy, S.A.R. (eds) *Petroleum Geology of Northwest Europe: Proceedings of the 5th Conference*. Geological Society, London, 41–61.

Doré, A.G., Cartwright, J.A., Stoker, M.S., Turner, J.P. & White, N. 2002. Exhumation of the North Atlantic margin: introduction and background. *In:* Doré, A.G., Cartwright, J.A., Stoker, M.S., Turner, J.P. & White, N. (eds) *Exhumation of the North Atlantic Margin: Timing, Mechanisms and Implications for Petroleum Exploration*. Geological Society, London, Special Publications, **196**, 1–12.

Duddy, I.R., Green, P.F., Bray, R.J. & Hegarty, K.A. 1994. Recognition of the thermal effects of fluid flow in sedimentary basins. *In:* Parnell, J. (ed.) *Geofluids: Origin, Migration and Evolution of Fluids in Sedimentary Basins*. Geological Society, London, Special Publications, **78**, 325–345.

ELDRETT, J.S., HARDING, I.C., FIRTH, J.V. & ROBERTS, A.P. 2004. Magnetostratigraphic calibration of Eocene–Oligocene dinoflagellate cyst biostratigraphy from the Norwegian–Greenland Sea. *Marine Geology*, **204**, 91–127.

FALEIDE, J.I., KYRKJEBØ, R., KJENNERUD, T., GABRIELSEN, R., JORDT, H., FANAVOLL, S. & BJERKE, M.D. 2002. Tectonic impact on sedimentary processes during Cenozoic evolution of the northern North Sea and surrounding areas. *In:* DORÉ, A.G., CARTWRIGHT, J.A., STOKER, M.S., TURNER, J.P. & WHITE, N. (eds) *Exhumation of the North Atlantic Margin: Timing, Mechanisms and Implications for Petroleum Exploration*. Geological Society, London, Special Publications, **196**, 235–269.

FUNDER, S. & HANSEN, L. 1996. The Greenland ice sheet—a model for its culmination and decay during and after the last glacial maximum. *Bulletin of the Geological Society of Denmark*, **42**, 137–152.

GALBRAITH, R.F. & LASLETT, G.M. 1993. Statistical methods for mixed fission track ages. *Nuclear Tracks*, **21**, 459–470.

GALLAGHER, K. 1995. Evolving temperature histories from apatite fission-track data. *Earth and Planetary Science Letters*, **136**, 421–435.

GARDE, A.A. 1994. *Precambrian geology between Qarajaq Isfjord and Jakobshavn Isfjord, West Greenland. Geological map sheet, 1:250 000*. Geological Survey of Greenland, Copenhagen.

GEORGE, T.N. 1966. Geomorphic evolution in Hebridean Scotland. *Scottish Journal of Geology*, **2**, 1–34.

GIBSON, H. J., 1999. Thermal history reconstruction for six wells located west of Greenland using apatite fission track analysis and vitrinite reflectance. A report prepared for Phillips Petroleum company Norway, Stavanger. *Geotrack Report*, **732** (now open file).

GREEN, P.F. 1986. On the thermo-tectonic evolution of northern England: evidence from fission track analysis. *Geological Magazine*, **123**, 493–506.

GREEN, P.F. 1989. Thermal and tectonic history of the East Midlands shelf (onshore UK) and surrounding regions assessed by apatite fission track analysis. *Journal of the Geological Society, London*, **146**, 755–774.

GREEN, P.F. 2003. Thermal history reconstruction in the Ataa-1, Gane-1, Gant-1, Gro-3 and Umiivik-1 boreholes, onshore West Greenland, based on AFTA, vitrinite reflectance and apatite (U–Th)/He dating. A report prepared for GEUS by Geotrack International Pty Ltd. *Geotrack Report*, **883**.

GREEN, P.F. 2004. Burial and exhumation histories of Carboniferous rocks of the Southern North Sea and onshore UK, with particular emphasis on post-Carboniferous events. *In:* COLLINSON, J.D., EVANS, D.J., HOLLIDAY, D.W. & JONES, N.S. (eds) *Carboniferous Hydrocarbon Resources: the Southern North Sea and Surrounding Areas*. Yorkshire Geological Society Occasional Publications Series, **7**, 25–34.

GREEN, P.F., DUDDY, I.R., GLEADOW, A.J.W., TINGATE, P.R. & LASLETT, G.M. 1986. Thermal annealing of fission tracks in apatite 1. A qualitative description. *Chemical Geology (Isotope Geosciences Section)*, **59**, 237–253.

GREEN, P.F., DUDDY, I.R. & BRAY, J.R. 1995. Applications of thermal history reconstruction in inverted basins. *In:* BUCHANAN, J.G. & BUCHANAN, P.G. (eds) *Basin Inversion*. Geological Society, London, Special Publications, **88**, 149–165.

GREEN, P.F., DUDDY, I.R., BRAY, R.J., DUNCAN, W.I. & CORCORAN, D. 2001a. Thermal history reconstruction in the Central Irish Sea Basin. *In:* SHANNON, P.M., HAUGHTON, P.M. & CORCORAN, D. (eds) *Petroleum Exploration of Ireland's Offshore Basins*. Geological Society, London, Special Publications, **188**, 171–188.

GREEN, P.F., THOMSON, K. & HUDSON, J.D. 2001b. Recognising tectonic events in undeformed regions: contrasting results from the Midland Platform and East Midlands Shelf, Central England. *Journal of the Geological Society, London*, **158**, 59–73.

GREEN, P.F., DUDDY, I.R. & HEGARTY, K.A. 2002. Quantifying exhumation from apatite fission-track analysis and vitrinite reflectance data: precision, accuracy and latest results from the Atlantic margin of NW Europe. *In:* DORÉ, A.G., CARTWRIGHT, J.A., STOKER, M.S., TURNER, J.P. & WHITE, N. (eds) *Exhumation of the North Atlantic Margin: Timing, Mechanisms and Implications for Petroleum Exploration*. Geological Society, London, Special Publications, **196**, 331–354.

HALD, N. 1976. Early Tertiary flood basalts from Hareøen and western Nûgssuaq, West Greenland. *Bulletin Grønlands Geologiske Undersøgelse*, **120**, 36.

HANSEN, K. & BROOKS, C.K. 2002. The evolution of the East Greenland margin as revealed from fission-track studies. *Tectonophysics*, **349**, 93–111.

HENDRIKS, B.W.H. & ANDRIESSEN, P. 2002. Pattern and timing of the post-Caledonian denudation of northern Scandinavia constrained by apatite fission-track thermochronology. *In:* DORÉ, A.G., CARTWRIGHT, J.A., STOKER, M.S., TURNER, J.P. & WHITE, N. (eds) *Exhumation of the North Atlantic Margin: Timing, Mechanisms and Implications for Petroleum Exploration*. Geological Society, London, Special Publications, **196**, 117–137.

HENRIKSEN, N., HIGGINS, A.K., KALSBEEK, F. & PULVERTAFT, T.C.R. 2000. *Greenland from Archaean to Quaternary. Descriptive text to the geological map of Greenland, 1:2 500 000*. Geology of Greenland Survey Bulletin, **185**.

HURFORD, A.J.H. & GREEN, P.F. 1983. The zeta age calibration of fission-track dating. *Chemical Geology (Isotope Geosciences Section)*, **1**, 285–317.

JAPSEN, P. 1997. Regional Neogene exhumation of Britain and the western North Sea. *Journal of the Geological Society, London*, **154**, 239–247.

JAPSEN, P. 1998. Regional velocity–depth anomalies, North Sea Chalk: a record of overpressure and Neogene uplift and erosion. *AAPG Bulletin*, **82**, 2031–2074.

JAPSEN, P. & CHALMERS, J.A. 2000. Neogene uplift and tectonics around the North Atlantic: overview. *Global and Planetary Change*, **24**, 165–173.

JAPSEN, P., BIDSTRUP, T. & LIDMAR-BERGSTRÖM, K. 2002. Neogene uplift and erosion of southern Scandinavia induced by the rise of the South Swedish Dome. *In:* DORÉ, A.G., CARTWRIGHT, J.A., STOKER, M.S., TURNER, J.P. & WHITE, N. (eds) *Exhumation of the North Atlantic Margin: Timing, Mechanisms and Implications for Petroleum Exploration*. Geological Society, London, Special Publications, **196**, 183–207.

JOHNSON, C. & GALLAGHER, K. 2000. Preliminary Mesozoic and Cenozoic denudation history of the North East Greenland onshore margin. *Global and Planetary Change*, **24**, 261–274.

JONES, S.M., WHITE, N., CLARKE, B.J., ROWLEY, E. & GALLAGHER, K. 2002. Present and past influence of the Iceland Plume on sedimentation. *In:* DORÉ, A.G., CARTWRIGHT, J.A., STOKER, M.S., TURNER, J.P. & WHITE, N. (eds) *Exhumation of the North Atlantic Margin: Timing, Mechanisms and Implications for Petroleum Exploration*. Geological Society, London, Special Publications, **196**, 13–25.

LARSEN, H.C., SAUNDERS, A.D. & CLIFT, P.D. *ET AL.* 1994. Seven million years of glaciation in Greenland. *Science*, **264**, 952–955.

LIDMAR-BERGSTRÖM, K. & NÄSLUND, J.O. 2002. Landforms and uplift in Scandinavia. *In:* DORÉ, A.G., CARTWRIGHT, J.A., STOKER, M.S., TURNER, J.P. & WHITE, N. (eds) *Exhumation of the North Atlantic Margin: Timing, Mechanisms and Implications for Petroleum Exploration*. Geological Society, London, Special Publications, **196**, 103–116.

MATHIESEN, A. 1998. *Modelling of uplift history from maturity and fission track data, Nuussuaq, West Greenland*. Danmarks og Grønlands Geologiske Undersøgelse Rapport, **1998/87**.

MATHIESEN, A., BIDSTRUP, T. & CHRISTIANSEN, F.G. 2000. Denudation and uplift history of the Jameson Land basin, East Greenland—constrained from maturity and apatite fission data. *Global and Planetary Change*, **24**, 275–301.

NEWMAN, J. 1997. New approaches to the detection and correction of suppressed vitrinite reflectance. *APPEA Journal*, **27**, 524–535.

NIELSEN, S.B., PAULSEN, G.E. & HANSEN, D.L. *ET AL.* 2002. Paleocene initiation of Cenozoic uplift in Norway. *In:* DORÉ, A.G., CARTWRIGHT, J.A., STOKER, M.S., TURNER, J.P. & WHITE, N. (eds) *Exhumation of the North Atlantic Margin: Timing, Mechanisms and Implications for Petroleum Exploration*. Geological Society, London, Special Publications, **196**, 45–65.

NØHR-HANSEN, H. 1997. *Palynology of the Gro-3 well, Nuussuaq, West Greenland*. Danmarks og Grønlands Geologiske Undersøgelse Rapport, **1997/151**.

NØHR-HANSEN, H. 2003. Dinoflagellate cyst stratigraphy of the Palaeogene strata from the Hellefisk-1, Ikermiut-1, Kangâmiut-1, Nukik-1, Nukik-2 and Qulleq-1 wells, offshore West Greenland. *Marine and Petroleum Geology*, **19**, 1–30.

NØHR-HANSEN, H., SHELDON, E. & DAM, G. 2002. A new biostratigraphic scheme for the Paleocene onshore West Greenland and its implications for the timing of the pre-volcanic evolution. *In:* JOLLEY, D.W. & BELL, B.R. (eds) *The North Atlantic Igneous Province: Stratigraphy, Tectonic, Volcanic and Magmatic Processes*. Geological Society, London, Special Publications, **197**, 111–156.

PEDERSEN, A.K., LARSEN, L.M. & DUEHOLM, K.S. 1993. *Geological section along the south coast of Nuussuaq, central West Greenland, 1: 20 000, coloured geological sheet*. Geological Survey of Greenland, Copenhagen.

PEDERSEN, A.K., LARSEN, L.M. & DUEHOLM, K.S. 2002a. *Geological section along the north side of the Aaffarsuaq valley and central Nuussuaq, central West Greenland, 1:20 000, coloured geological sheet*. Geological Survey of Denmark and Greenland, Copenhagen.

PEDERSEN, A.K., LARSEN, L.M., RIISAGER, P. & DUEHOLM, K.S. 2002b. Rates of volcanic deposition, facies changes and movements in a dynamic basin: the Nuussuaq Basin, West Greenland, around the C27n–C26R transition. *In:* JOLLEY, D.W. & BELL, B.R. (eds) *The North Atlantic Igneous Province: Stratigraphy, Tectonic, Volcanic and Magmatic Processes*. Geological Society, London, Special Publications, **197**, 157–181.

PIASECKI, S. 2003. Neogene dinoflagellate cysts from Davis Strait, offshore West Greenland. *Marine and Petroleum Geology*, **20**, 1075–1088.

PIASECKI, S., LARSEN, L.M., PEDERSEN, A.K. & PEDERSEN, G.K. 1992. Palynostratigraphy of the lower Tertiary volcanics and marine clastic sediments in the southern part of the West Greenland Basin: implications for the timing and duration of the volcanism. *Rapport Grønlands Geologiske Undersøgelse*, **154**, 13–31.

RIIS, F. & FJELDSKAAR, W. 1992. On the magnitude of the late Tertiary and Quaternary erosion and its significance for the uplift of Scandinavia and the Barents Sea. *In:* LARSEN, R.M., BREKKE, H., LARSEN, B.T. & TELLERAAS, E. (eds) *Structural and Tectonic Modelling and its Application to Petroleum*

Geology. Norwegian Petroleum Society Special Publications, **1**, 163–185.

Riisager, P. & Abrahamsen, N. 1999. Magnetostratigraphy of Paleocene basalts from the Vaigat Formation of West Greenland. *Geophysical Journal International*, **137**, 774–782.

Rohrman, M. & van der Beek, P. 1996. Cenozoic postrift domal uplift of North Atlantic margins: an asthenospheric diapirism model. *Geology*, **24**, 901–904.

Rohrman, M., van der Beek, P., Andriessen, P. & Cloetingh, S. 1995. Meso-Cenozoic morphotectonic evolution of southern Norway: Neogene domal uplift inferred from apatite fission track thermochronology. *Tectonics*, **14**, 704–718.

Rohrman, M., van der Beek, P., van der Hilst, R.D. & Reemst, P. 2002. Timing and mechanics of North Atlantic Cenozoic uplift; evidence for mantle upwelling. *In:* Doré, A.G., Cartwright, J.A., Stoker, M.S., Turner, J.P. & White, N. (eds) *Exhumation of the North Atlantic Margin: Timing, Mechanisms and Implications for Petroleum Exploration*. Geological Society, London, Special Publications, **196**, 27–43.

Rolle, F. 1985. Late Cretaceous–Tertiary sediments offshore central West Greenland: lithostratigraphy, sedimentary evolution, and petroleum potential. *Canadian Journal of Earth Sciences*, **22**, 1001–1019.

Rosenkrantz, A., Münther, V. & Henderson, G. 1974. *Geological map of Greenland, 1:100 000, Agatdal 70 V.* Geological Survey of Greenland, Copenhagen, **1**.

Skaarup, N. 2002. Evidence for continental crust in the offshore Palaeogene volcanic province, central West Greenland. *Geology of Greenland Survey Bulletin*, **191**, 97–102.

Srivastava, S.P. & Keen, C.E. 1995. A deep seismic reflection profile across the mid-Labrador spreading centre. *Tectonics*, **14**, 372–389.

Stoker, M.S. 2002. Late Neogene development of the UK Atlantic margin. *In:* Doré, A.G., Cartwright, J.A., Stoker, M.S., Turner, J.P. & White, N. (eds) *Exhumation of the North Atlantic Margin: Timing, Mechanisms and Implications for Petroleum Exploration*. Geological Society, London, Special Publications, **196**, 313–329.

Stoker, M.S., Praeg, D. & Shannon, P.M. *et al*. 2005. Neogene evolution of the Atlantic continental margin of NW Europe (Lofoten Islands to SW Ireland): anything but passive. *In:* Doré, A.G. & Vining, B. (eds) *Petroleum Geology: NW Europe and Global Perspectives: Proceedings of the 6th Conference*. Geological Society, London, 1057–1076.

Storey, M., Duncan, R.A., Pedersen, A.K., Larsen, L.M. & Larsen, H.C. 1998. $^{40}Ar/^{39}Ar$ geochronology of the West Greenland Tertiary volcanic province. *Earth and Planetary Science Letters*, **160**, 569–586.

Stuevold, L.M. & Eldholm, O. 1996. Cenozoic uplift of Fennoscandia inferred from a study of the mid-Norwegian margin. *Global and Planetary Change*, **12**, 359–386.

Thomson, K., Green, P.F., Whitham, A.G., Price, S.P. & Underhill, J.R. 1999a. New constraints on the thermal history of North-East Greenland from apatite fission-track analysis. *Geological Society of America Bulletin*, **111**, 1054–1068.

Thomson, K., Underhill, J.R., Green, P.F., Bray, R.J. & Gibson, H.J. 1999b. Evidence from apatite fission track analysis for the post-Devonian burial and exhumation history of the northern Highlands, Scotland. *Marine and Petroleum Geology*, **16**, 27–39.

White, N. & Lovell, B. 1997. Measuring the pulse of a plume with the sedimentary record. *Nature*, **387**, 888–891.

Wilkins, R.W.T., Wilmshurst, J.R., Russell, N.J., Hladky, G., Ellacott, M.V. & Buckingham, C. 1992. Fluorescence alteration and the suppression of vitrinite reflectance. *Organic Geochemistry*, **18**, 629–640.

Received 31 March 2004; revised typescript accepted 10 August 2004.
Scientific editing by Rob Strachan